Materials Transactions, Vol. 66, No. 7 (2025) pp. 907 to 911

RAPID PUBLICATION

Effect of Loading Direction on Compression Behaviour of Pure Magnesium at Different Grain-Size and Strain-Rates

Elango Chandiran*, Yukiko Ogawa, Rintaro Ueji and Hidetoshi Somekawa

Research Center for Structural Materials, National Institute for Materials Science, Tsukuba 305-0047, Japan

This study investigates the effect of loading direction on the compression behaviour of extruded pure magnesium with different grain-sizes and at different strain-rate. At the same grain-size level, samples compressed at 45 degrees to the extrusion direction have lower yield stress than samples compressed parallel to the extrusion direction. However, the loading direction has a negligible effect on the dominant deformation modes in the studied conditions. [doi:10.2320/matertrans.MT-M2025008]

(Received January 27, 2025; Accepted March 24, 2025; Published April 18, 2025)

Keywords: *pure magnesium, grain-size, loading direction, compression, flow stress*

1. Introduction

Wrought processing of magnesium (Mg) and its alloys results in the development of a strong crystallographic texture, which significantly affects its room-temperature formability and limits their use in commercial applications [1, 2]. It has been shown that modifying the crystallographic texture can improve the formability and specific strength-ductility balance of Mg and its alloys [2, 3]. The changes in initial texture caused by variations in the angle between the loading direction and the *c*-axis of the crystal, can activate different deformation mechanism [4]. The activation of non-basal slip mechanisms promotes more homogenous deformation, improving ductility [5]. Peng *et al.* [6], in an extruded AZ31 Mg alloy, showed that the dominant deformation modes changed gradually during compression, with more pronounced increase in the angle between the loading direction and the *c*-axis during the tension testing.

In addition to texture and loading direction, other factors, such as grain-size and strain-rates, significantly influence the deformation behaviour of Mg alloys [4–8]. For instance, grain boundary sliding (GBS) is observed at room-temperature in a fine grain-size structures, particularly at lower strain-rates [7, 8]. However, the contribution of GBS is to overall ductility remain limited, as dislocation slip remains the dominant deformation mechanism in the extruded Mg at room-temperature [8]. Moreover, the influence of loading direction on the deformation behaviour further complicates the materials response in extruded samples. Despite advances in understanding the effects of loading direction, grain-size, and strain-rate on deformation behaviour, their combined effect is not well understood. This study investigates how loading direction, grain-size, and strain-rate influence the compression behaviour of pure Mg at room-temperature, focusing on yield stress and deformation modes to identify factors that could improve the mechanical properties of Mg alloys.

*Corresponding author, E-mail: CHANDIRAN.elango@nims.go.jp

2. Materials and methods

Commercial grade pure Mg (99.96% purity) was used in this study. The cast pure Mg was extruded into bar of 8 mm in diameter at 623 K, 423 K, and 378 K with an extrusion ratio of 25:1 at an extrusion speed of 0.2 mm/s. From the extruded bars, cylindrical samples with compression axis (CA) parallel to the extrusion direction, (ED) (referred to as CA//ED) and 45° to the extrusion direction (referred to as CA//45°ED) were prepared. The sample size was either 4 mm in diameter and 8 mm in height or 3 mm in diameter and 6 mm in height. These samples were compressed at room-temperature at strain-rates of $1 \times 10^{-3}\,s^{-1}$, $1 \times 10^{-4}\,s^{-1}$ and $1 \times 10^{-5}\,s^{-1}$. For selected deformation conditions, the samples were compressed to intermediate strains ranging from 0.08 to 0.12. The microstructures of the samples were examined in a plane parallel to the compression axis using a scanning electron microscope equipped with a backscatter electron detector. For microscopic observation, the samples were mechanically polished and etched in a 6% aqueous solution of hydrochloric acid. The detailed sample preparation methods for microstructure observation have been reported elsewhere [8].

3. Results and Discussion

Figure 1 shows representative microstructure and inverse pole figure triangles along the compression axis (CA) of samples with CA//ED and CA//45°ED. The microstructural features, obtained from statistically sufficient EBSD measurements, show equiaxed grains, with grain-size decreasing as the extrusion temperature decreases. In the coarse grain-size ($d = 88\,\mu m$) sample with CA//ED, the $\langle 10\bar{1}0\rangle$ direction of grains are predominantly parallel to the CA, followed by $\langle 2\bar{1}\bar{1}0\rangle$ (Fig. 1(b)). This indicates that the basal *c*-axes of most grains are nearly perpendicular to the CA which suggest a basal texture. On the other hand, in the sample with CA//45°ED (Fig. 1(c)), the grains were random along the loading direction. Similar behaviour is observed with decreasing the grain-size (Fig. 1(d)–(i)). Therefore, observable differences in the compression behaviour of these samples can be solely attributed primarily to the grain-size.

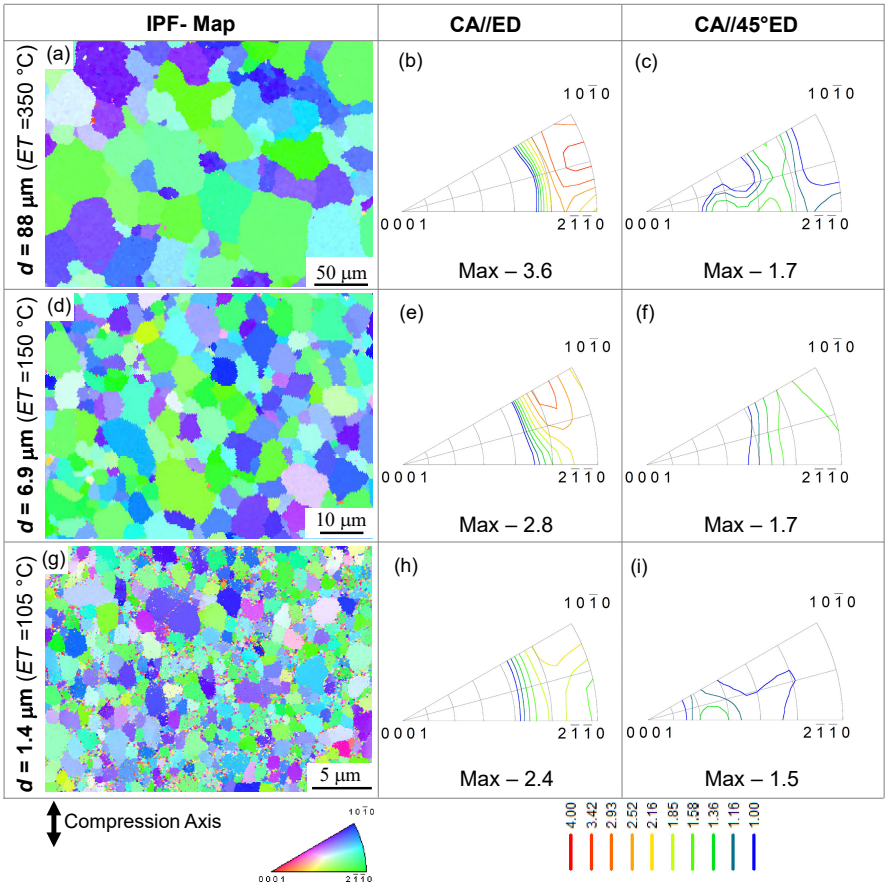

Fig. 1 (a) Inverse pole figure (IPF) map, (b) IPF triangles along compression axis parallel to extrusion direction (CA//ED) and (c) IPF triangles along compression axis 45° to extrusion direction (CA//45°ED) for coarse grain-size sample ($d = 88\,\mu m$); Similarly (d), (e) and (f) for meso grain-size sample ($d = 6.9\,\mu m$); and (g), (h) and (i) for fine grain-size sample ($d = 1.4\,\mu m$); ET: extrusion temperature; ED: extrusion direction; CA: compression axis. (online color)

Figure 2, summarizes the compression behaviour of the samples. Note that the stress-strain curves for the coarse ($d = 88\,\mu m$) and fine ($d = 1.4\,\mu m$) grain-size samples with CA//ED are adapted from our previous work [8]. For the same grain-size level, both the yield stress and the maximum strength are lower in samples with CA//45°ED than samples with CA//ED (Fig. A1(a)). At a strain-rate of $1 \times 10^{-3}\,s^{-1}$, strain hardening is observed after yielding in both coarse grain-size ($d = 88\,\mu m$) and meso grain-size ($d = 6.8\,\mu m$) samples with CA//45°ED (Fig. 2(a)). On the other hand, the strain hardening is less significant after yielding in the fine grain-size sample ($d = 1.4\,\mu m$) (Fig. 2(a)). The decrement in strain hardening with grain refinement observed in the CA//45°ED samples is similar to that observed in the CA//ED samples. At a strain-rate of $1 \times 10^{-5}\,s^{-1}$, the stress-strain behaviour of the CA//45°ED sample is again similar to that of the CA//ED samples (Fig. 2(b)).

Figure 2(c) shows the variations in flow stress at 0.02 plastic strain for different strain-rates. At strain-rates above $1 \times 10^{-4}\,s^{-1}$, the flow stress increases with grain refinement at the same strain-rate. Additionally, for the same grain-size level, the flow stress is lower in samples with CA//45°ED compared to those with CA//ED. For grain-sizes smaller than 6.8 µm, the flow stress decreases significantly as strain-rates are reduced. At strain-rates below $1 \times 10^{-4}\,s^{-1}$, the decrease in the flow stress is considerably increased in the fine grain samples ($d = 1.4\,\mu m$). The variation of flow stress at different strain-rate is similar to the yield stress (Fig. A1(a)). Moreover, the yield stress of the fine grain sample ($d = 1.4\,\mu m$) at low strain-rate ($1 \times 10^{-5}\,s^{-1}$) are comparable to that of the coarse grain-size ($d = 88\,\mu m$) and meso grain-size ($d = 6.9\,\mu m$) samples.

These results demonstrated that both yield and flow stress are strongly influenced by loading direction, grain-size, and strain-rates. However, in terms of the slope of strain-rate vs flow stress, no significant difference is observed between samples with CA//45°ED and those with CA//ED. Since the slope of strain-rates vs flow stress is related to strain-rate sensitivity factor (m) [9], the similar slope observed in both CA//45°ED and CA//ED sample sets, suggest that the that dominant deformation modes are less likely to be influenced by the loading direction during compression.

Figure 3 summarizes the deformation behaviour during compression of pure Mg with CA//45°ED. At a strain-rate of $1 \times 10^{-3}\,s^{-1}$, the formation of deformation twins is frequently observed in the coarse grain-size sample ($d = 88\,\mu m$) (Fig. 3(a)). On the other hand, in the fine grain-size sample, such deformation twins are not observed (Fig. 3(b)). This suggest that grain refinement retards the formation of deformation twins since grain refinement is known to increase the stress required for deformation twin formation [10].

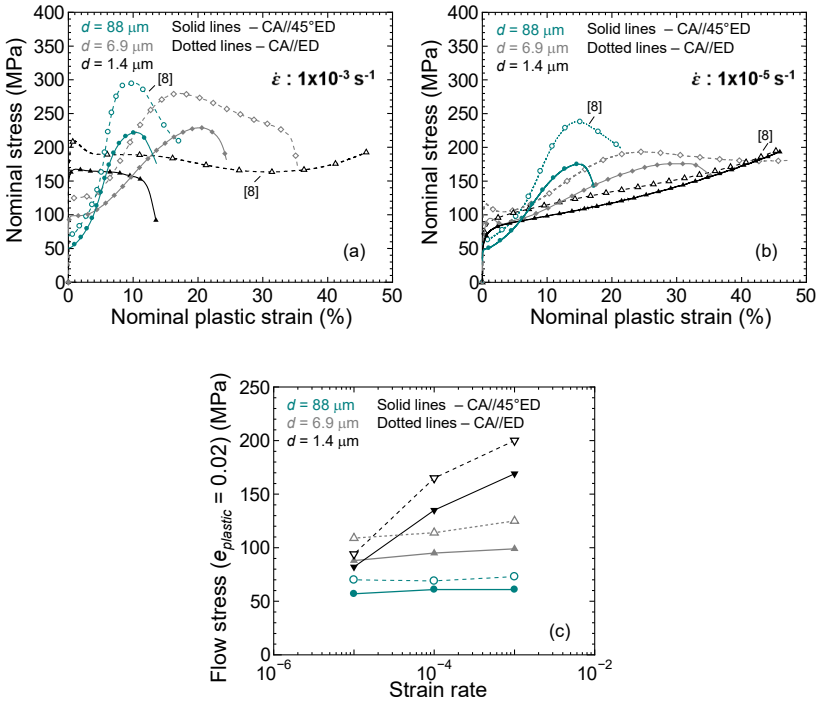

Fig. 2 Nominal stress-plastic strain curves at strain-rates (a) $1 \times 10^{-3}\,s^{-1}$ and (b) $1 \times 10^{-5}\,s^{-1}$; (c) variation in flow stress at different strain-rates. (online color)

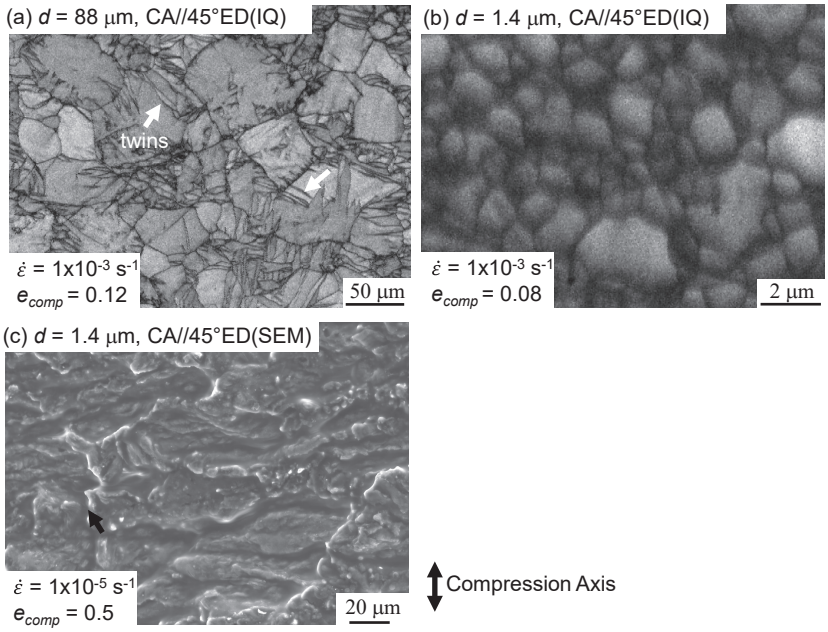

Fig. 3 Image quality map (IQ) of sample with CA//45°ED at $1 \times 10^{-3}\,s^{-1}$ grain (a) coarse grain-size sample ($d = 88\,\mu m$) after strain of 0.12, (b) fine grain-size sample ($d = 1.4\,\mu m$) after strain of 0.08, (c) SEM image of deformed surface of fine grain-size sample with CA//45°ED at $1 \times 10^{-5}\,s^{-1}$.

At a strain-rate of $1 \times 10^{-5}\,s^{-1}$, the formation of the deformation twin is confirmed in the coarse grain-size sample ($d = 88\,\mu m$) with CA//45°ED (Fig. A1(b)). At a strain of 0.10, the twin fraction (f_{twin}) was determined as 0.17, which is similar to that of a coarse grain-size sample ($d = 88\,\mu m$) with CA//ED ($f_{twin} = 0.16$). In the fine grain-size sample ($d = 1.4\,\mu m$) with CA//45°ED, deformation twins are not observed (Fig. A1(c)). Furthermore, the surface of the fine grain-size sample ($d = 1.4\,\mu m$) with CA//45°ED, exhibits wavy-like features (Fig. 3(c)), which are attributable to the GBS effect [7]. For Mg, m-values over 0.2 is reported to indicate a contribution from GBS to overall deformation at room-temperature [11]. In the fine grain-size sample ($d = 1.4\,\mu m$) with CA//ED an m-value ≥ 0.3, was observed at strain-rates below ($1 \times 10^{-4}\,s^{-1}$), demonstrating further contribution from GBS [8]. In the fine grain-size sample ($d = 1.4\,\mu m$) with CA//45°ED, similar slopes were observed as in the case of the CA//ED sample (Fig. A1(a)). These

results suggests that in fine grain-size sample ($d = 1.4\,\mu m$) CA//45°ED dislocation slip dominates deformation behaviour, with GBS also contributing at low strain-rate ($1 \times 10^{-5}\,s^{-1}$). At strain-rates over $1 \times 10^{-4}\,s^{-1}$, the *m*-value decreases, leading to a lesser contribution from GBS, and the overall deformation is dominated by dislocation slip [12].

In contrast, in the coarse grain-size samples ($d = 88\,\mu m$), deformation is dominated by dislocation slip and twinning, irrespective of loading direction. Similar results were reported by Peng *et al.* [6], where for compression at 0° to 61.9° from the extrusion direction of AZ31 with grain-size 13 μm, deformation mechanism is dominated by basal slip and twinning in large volume fraction of grains. It is evident that the loading direction has a less significant effect on the dominant deformation modes during room-temperature compression behaviour of extruded pure Mg, whereas grain-size has a significant influence.

The deformation modes of pure Mg at ambient-temperature include dislocation slip on the basal, prismatic, and pyramidal planes, as well as twinning. Among these modes, basal slip is the primary deformation mode in polycrystalline magnesium due to its typically lower critical resolved shear stress (CRSS) required for activation [13, 14]. Consequently, the yield stress is strongly influenced by the activation of basal slip, which is significantly dependent on the angular relationship between the mechanical loading direction and the crystallographic texture in wrought Mg [6, 14]. According to the Schmid law for a single crystal, the yield stress is inversely proportional to the critical resolved shear stress for a given direction [15].

To understand the effect of loading direction on the yield stress, the number fraction distribution of the Schmid factor (for basal slip) was determined for samples with CA//45° ED and CA//ED for both coarse grain-size ($d = 88\,\mu m$) (Fig. 4(a)) and fine grain-size ($d = 1.4\,\mu m$) (Fig. 4(b)). As, the change in loading directions (with CA//45°ED and CA//ED) was prepared by cutting the extruded samples at 0° and 45° relative to the extrusion direction. The samples were fully recrystallized structures (Fig. 1). This suggests that changes in the yield stress is primary influenced by the loading direction and grain-size.

In the coarse grain-size sample ($d = 88\,\mu m$) with CA//45° ED, a large fraction of grains exhibits a higher Schmid factor for basal slip compared to the samples with CA//ED (Fig. 4(a)). The average Schmid factor for basal slip in the sample with CA//45° ED is 0.33 (as shown in the inserted table), which is higher than that in the sample with CA//ED (0.16). In the fine grain-size sample ($d = 1.4\,\mu m$) with CA//45°ED, a larger fraction of grains also exhibits higher Schmid factors for basal slip than the sample with CA//ED. This explains the observed lower yield stress in the sample with CA//45°ED compared to the sample with CA//ED (Figs. 1(a), 1(b) and Fig. A1(a)). Most grains in the CA//45°ED sample are oriented such that basal slip is readily activated upon compression. These results suggest that, for the same grain-size, the loading direction significantly affects the yield stress in extruded bars of pure Mg (i.e., for samples with the same grain-size, CA//45°ED results in lower yield stress than CA//ED). Furthermore, it is noteworthy that dislocation-slip is primarily responsible for the initiation of yielding, irrespective of grain-size, strain-rate, or loading direction.

4. Conclusion

The effect of loading directions on the room-temperature compression behavior of extruded pure Mg with different grain-sizes was investigated. The loading direction affects yield stress, with samples compressed at 45° to the extrusion direction having lower yield stress. This lower yield stress is due to a higher proportion of grains with a high Schmid factor for basal slip. In the coarse grain sample ($d = 88\,\mu m$), the deformation mode was dominated by slip and deformation twinning. On the other hand, in a fine grain sample ($d = 1.4\,\mu m$), the deformation is dominated by slip, and at low strain-rate ($1 \times 10^{-5}\,s^{-1}$), in addition to slip, grain boundary sliding also contributes to the deformation behavior. Furthermore, in the studied conditions, the dominant deformation modes were found to be less affected by the loading direction during room-temperature compression of pure Mg.

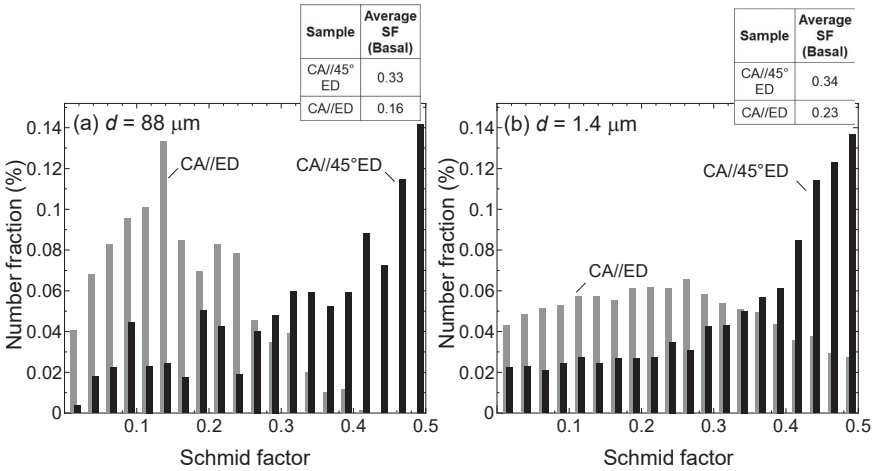

Fig. 4 Number fraction distribution of Schmid factor for basal slip in (a) coarse grain-size sample ($d = 88\,\mu m$) and (b) fine grain-size sample ($d = 1.4\,\mu m$).

REFERENCES

[1] T.T.T. Trang, J.H. Zhang, J.H. Kim, A. Zargaran, J.H. Hwang, B.-C. Suh and N.J. Kim: Designing a magnesium alloy with high strength and high formability, Nat. Commun. **9** (2018) 2522.

[2] J.F. Nie, K.S. Shin and Z.R. Zeng: Microstructure, deformation, and property of wrought magnesium alloys, Metall. Mater. Trans. A **51** (2020) 6045–6109.

[3] T. Mukai, M. Yamanoi, H. Watanabe and K. Higashi: Ductility enhancement in AZ31 magnesium alloy by controlling its grain structure, Scr. Mater. **45** (2001) 89–94.

[4] Y. Wang and H. Choo: Influence of texture on Hall–Petch relationships in an Mg alloy, Acta Mater. **81** (2014) 83–97.

[5] R. Gehrmann, M.M. Frommert and G. Gottstein: Texture effects on plastic deformation of magnesium, Mater. Sci. Eng. A **395** (2005) 338–349.

[6] J. Peng, Z. Zhang, H. Chen, C. Long, Y. Wu, W. Zhou and Y. Wu: Investigation on the anisotropy of mechanical properties along different orientations of an AZ31 hot-extrusion bar, J. Alloy. Compd. **854** (2021) 157108.

[7] H. Somekawa, A. Singh, R. Sahara and T. Inoue: Excellent room temperature deformability in high strain rate regimes of magnesium alloy, Sci. Rep. **8** (2018) 656.

[8] E. Chandiran, Y. Ogawa, R. Ueji and H. Somekawa: An inverse Hall-Petch relationship during room-temperature compression of commercially pure magnesium, J. Alloy. Compd. **930** (2023) 167443.

[9] M. Barnett, Z. Keshavarz, A. Beer and D. Atwell: Influence of grain size on the compressive deformation of wrought Mg–3Al–1Zn, Acta Mater. **52** (2004) 5093–5103.

[10] F.A. Nichols: Plastic instabilities and uniaxial tensile ductilities, Acta Metall. **28** (1980) 663–673.

[11] Z. Zeng, J.F. Nie, S.W. Xu, C.H.J. Davies and N. Birbilis: Superformable pure magnesium at room temperature, Nat. Commun. **8** (2017) 972–977.

[12] H. Somekawa, A. Singh and T. Inoue: Development of Isotropic and Accordion-like Deformable Magnesium Alloys, Mater. Trans. **58** (2017) 1089–1092.

[13] H. Yoshinaga and R. Horiuchi: On the Flow Stress of α Solid Solution Mg-Li Alloy Single Crystals, Trans. JIM **4** (1963) 134–141.

[14] S. Kleiner and P.J. Uggowitzer: Mechanical anisotropy of extruded Mg–6% Al–1% Zn alloy, Mater. Sci. Eng. **379** (2004) 258–263.

[15] X.-L. Nan, H.-Y. Wang, L. Zhang, J.-B. Li and Q.-C. Jiang: Calculation of Schmid Factors in Magnesium: Analysis of Deformation Behaviors, Scr. Mater. **67** (2012) 443–446.

Appendix

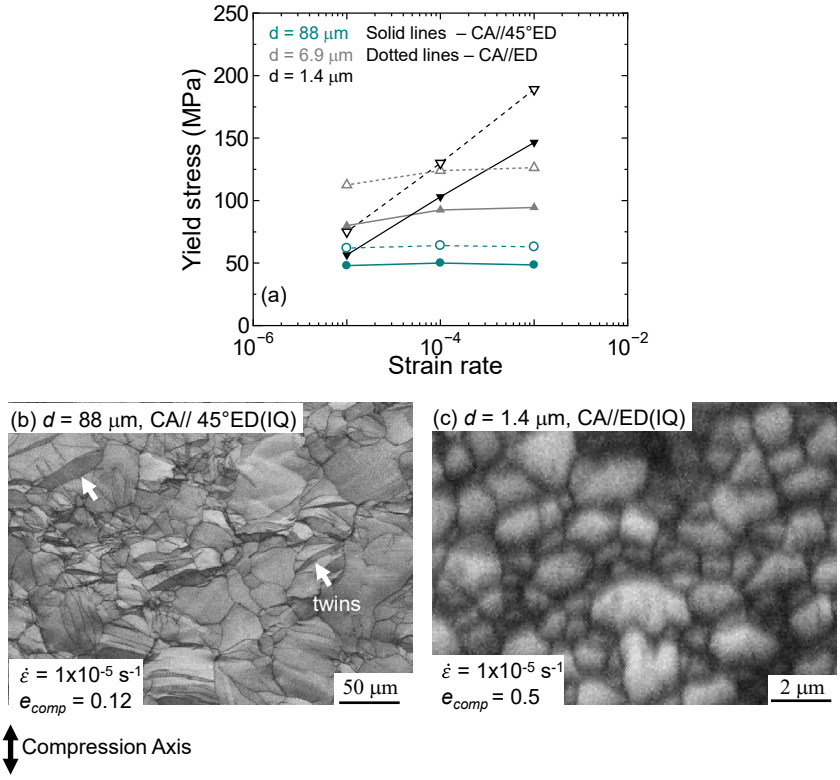

Fig. A1 (a) Variation in yield stress at different strain-rates. IQ map of sample with CA//45°ED at $1 \times 10^{-5}\,s^{-1}$ (b) coarse grain-size sample ($d = 88\,\mu m$) after strain of 0.12, (c) fine grain-size sample ($d = 1.4\,\mu m$) compressed to strain of 0.5. (online color)